

3D numerical investigation on the interaction between mechanized twin tunnels in soft ground

Ngoc-Anh Do · Daniel Dias · Pierpaolo Oreste

Received: 28 February 2014 / Accepted: 18 July 2014 / Published online: 1 August 2014
© Springer-Verlag Berlin Heidelberg 2014

Abstract During the construction of twin tunnels excavated in close proximity to each other, the prediction of the influence of a new tunnel construction on an already existing one plays an important role in the design and construction of the tunnels. The researches in the literature indicate that this influence depends to a great extent on the distance between the tunnels. However, most of the reported cases in the literature on the mechanized excavation of twin tunnels have focused on the effects of the relative position between the two tunnels on surface settlements. Some of them have dealt with the behaviour of the tunnel structure through the use of simplified numerical models. The numerical investigation performed in this study, using the FLAC^{3D} finite difference code, has made it possible to predict the impact between tunnels using full three-dimensional simulations, in which most of the elements of a mechanized tunnel process have been modelled. The effects of tunnel distance on the structural forces induced in both tunnels, and the displacements in the surrounding ground have been highlighted. A modification has

been made to the superposition method to predict the settlement surface trough over twin tunnels.

Keywords Numerical modelling · Lining response · Segmental lining · Settlement · Tunnel distance · Twin tunnel

Introduction

The number of twin tunnels excavated in close proximity to each other using the mechanized method has recently been increasing due to the expansion of transportation in large cities. Through an examination of surface settlements over twin tunnels, which were excavated by means of the Earth pressure balance (EPB) shield method in the Istanbul Metro Line, Ocak (2009) showed that the control of surface settlements during tunnelling in urbanized areas is very important, in terms of preventing damage to existing buildings and infrastructures. In addition, the prediction of the effect of a new shield tunnel construction on the tunnel lining of an existing tunnel also plays an important role in the optimal design of close parallel shield tunnels.

A review of twin tunnel interaction has been given in a recent work by the authors of the present work (Do et al. 2014). Interactions between closely-spaced tunnels were studied in the past using a variety of approaches: physical model testing, field observations, empirical/analytical methods and finite element modelling. The literature reviewed in this work has clearly indicated that an extensive amount of research has been conducted on tunnel interactions between parallel tunnels. Most of the researches have so far focused on the effect of twin tunnel interaction on ground deformation. However, less work has been devoted to the influence of the interaction between

N.-A. Do
Laboratory LGCIE, INSA of Lyon, University of Lyon,
Villeurbanne, France

N.-A. Do
Department of Underground and Mining Construction, Faculty
of Civil Engineering, Hanoi University of Mining and Geology,
Hanoi, Vietnam

D. Dias (✉)
Laboratory LTHE, Grenoble Alpes University, Grenoble, France
e-mail: daniel.dias@ujf-grenoble.fr

P. Oreste
Department of Environmental, Land and Infrastructural
Engineering, Politecnico di Torino, Torino, Italy

tunnels on the structural forces induced in tunnel linings (Do et al. 2014).

Ocak and Seker (2013) predicted surface settlement over the twin EPB tunnels using three different methods: an artificial neural network, a support vector machine and Gaussian processes. This study considered 18 different parameters, that is, EPB operation factors, geometric properties of the tunnel and ground properties. He indicated that the most effective parameters for surface settlement prediction are the amount of excavated material, the percentage of tail void grouting filling, the depth of the tunnel, the face pressure and the distance between the two tunnels.

On the basis of measurement data on ground movements induced by parallel EPB tunnels excavated in soft ground in Bangkok, Suwansawat and Einstein (2007) proposed a superposition technique procedure to describe the settlement trough that develops over twin horizontal tunnels using Gaussian curves. When the proposed superposition technique was used, the final total settlement troughs resulting from the twin tunnels were obtained. The superposition curves and the observed data were in very good agreement. Their results also showed that the maximum settlement for twin tunnels is not usually located over the centreline of the pillar between two tunnels, and that the settlement trough is often asymmetric.

Using the superposition method, Ocak (2014) has presented a new equation to estimate the transverse settlement curve for twin EPB tunnels. A disturbance factor, which depends on the diameter of the tunnel and the lateral distance between the two tunnels, is used to consider the fact that the second tunnel is excavated in soil disturbed by the excavation of the first tunnel. The proposed equation was validated against number of field observations. It should be noted that the transverse settlement troughs obtained in this study incline toward the second tunnel.

Chen et al. (2012) have conducted two-dimensional (2D) numerical investigations in order to estimate the applicability of the superposition method in predicting the ground surface settlements of twin and quadruple tunnels. On the basis of a comparison with experimental data obtained from the Taipei Rapid Transit System, which was mainly excavated using shield machines, the results indicated that the ground surface settlement profile of a multi-tube tunnel could be conveniently and reliably estimated using the empirical equation together with the principle of superposition. However, it should be noted that certain elements of a mechanized tunnelling process, such as face pressure, grouting pressure, jacking force, displacement in the shield zone, etc., were not taken into consideration in their study.

Through the use of 2D numerical calculations, Hage Chehade and Shahrour (2008) have shown that, the construction of the first tunnel, beyond a distance from the

centre to the centre of three times the tunnel diameter, does not affect the second one. The same conclusion can be drawn from the work performed by Do et al. (2013b). However, the critical distance obtained through 2D investigations by Hefny et al. (2004) was about 2.5 times the tunnel diameter. The difference in the results obtained in the literature could be attributed to the fact that, when 2D numerical calculations were performed in these works, different simplified methods were used to take the three-dimensional (3D) effect of the tunnelling process into account. An interesting estimation on the effect of the tunnel distance on twin tunnel interaction, which was obtained on the basis of field measurements conducted in EPB tunnel sites, can be seen in the work by Ocak (2014). In this case, the effect of the first tunnel excavation on the development of a settlement curve over the second tunnel, which was represented through the use of a disturbance factor, was even significant at a distance from the centre to the centre of 9 times the tunnel diameter. However, 3D calculations are obviously necessary for an effective estimation of the interaction between two tunnels.

Chakeri et al. (2011) performed a 3D numerical investigation that showed the changes in stress distribution, deformations and surface settlements of twin metro tunnels in Tehran. The horseshoe shaped tunnels are supported by shotcrete and lattice girders. The spacing effect between the tunnels and the effect of the excavation sequence on the surface settlements were highlighted. Ercelebi et al. (2011) presented an interesting comparison of three settlement prediction methods for mechanized tunnel excavation, that is, numerical analysis with the finite element method, analytical method and semi-theoretical (semi-empirical) methods. The results of the predictions were compared and verified by means of field measurements, and a good agreement emerged between these methods.

The work conducted by Do et al. (2014) has focused on the study of the behaviour of the interaction of mechanized twin tunnels, in terms of the structural forces induced in the tunnel lining and the ground displacements surrounding the two tunnels. Most of the main elements of a mechanized excavation have been simulated in this model. The CYsoil model (Itasca 2009), which is a strain-hardening constitutive model, has been adopted. However, only a distance of 1.25D, with D the tunnel diameter, from the centre to the centre of the tunnels has been considered in this work. The numerical analysis has indicated an important impact of the new tunnel construction on the existing one. The influence of the lagged distance between the two tunnel faces has also been highlighted. Generally, the simultaneous excavation of twin tunnels causes smaller structural forces and lining displacements than those induced in the case of twin tunnels excavated at a large lagged distance. However, the

simultaneous excavation of twin tunnels could result in a higher settlement above the two tunnels.

On the basis of the full 3D numerical model developed in the aforementioned work by the same authors (Do et al. 2014), the present study has the aim of highlighting the effect of the tunnel distance between two horizontal tunnels on their structural behaviour and the displacements of the ground surrounding the tunnels. A modification of the superposition method introduced by Suwansawat and Einstein (2007) is presented. The Bologna-Florence high speed railway line has been adopted in this study as a reference case.

Numerical model

FLAC^{3D} (fast Lagrange analysis of continua in three-dimensions) (Itasca 2009), which is based on the finite difference method, has been used for the numerical modelling in this study. Basically, the same 3D numerical model that was used in the work by the same authors (Do et al. 2014) has been adopted in the present study. All the parameters of the numerical model are similar to those illustrated in Do et al. (2013a, 2014). Therefore, only a short overview is given here.

Parameters from the Bologna-Florence high speed railway line project, which is part of the Italian high speed railway network, have been used in this study for reference purpose. The twin horizontal tunnels, with a space distance of 15 m from the centre to the centre, have an external excavation diameter (D) of 9.4 m and an internal diameter of 8.3 m. The tunnels were excavated at a depth of between 15 and 25 m below the ground surface, through two main formations: alluvial deposit of the late Pleistocene–Pliocene era, which is mostly made up of alluvial deposits from the Savena River with deposits of clay, and sandy soil (clayey sands and Pliocene clay). Some typical parameters of ring 582 section have been adopted in this study (see Do et al. 2013a).

The soil has been simulated using the CYsoil constitutive model (Itasca 2009), which is a strain-hardening constitutive model. This constitutive model is characterized by a frictional Mohr–Coulomb shear envelope (zero cohesion) and an elliptic volumetric cap in the (p' , q) plane.

The tunnel construction process has been modelled using a step-by-step approach. Each excavation step corresponds to an advancement of 1.5 m of the tunnel face, which is equal to the width of a lining ring installed at the shield tail location. The tunnelling process consists of three main phases (Do et al. 2013a):

- Excavating the ground at the tunnel face and simultaneously applying a confinement to ensure tunnel face stability.
- Installing the tunnel lining, applying the jacking force and injecting the grout behind the segments in order to fill the voids created at the shield tail.
- The shield machine continues to advance, and the ground begins to become stabilized, and this is expressed by a consolidation phase.

The face pressure applied to the excavation face from the shield chamber has been estimated on the basis of the horizontal stress induced in the ground in front of the tunnel face (Mollon et al. 2013). This face pressure distribution has been applied to the excavation face using a trapezoidal profile in order to account for the slurry density. A distributional radial pressure has also been applied to the cylindrical surface just behind the tunnel face. The shield machine has been simulated using the “fictive” shield illustrated by Dias et al. (2000), Jenck and Dias (2004) and Mollon et al. (2013). The self-weight of the shield has been taken into account through the vertical loads acting on the grid points of the ground mesh at the bottom region of the tunnel over an assumed range of 90° in the cross-section, and over the whole shield length.

The jacking forces, which have been assumed to be linearly distributed over the height of the tunnel, were set on each segment of the last ring, considering three plates located at 1/6, 1/2 and 5/6 of the segment length.

The grouting layer has been modelled in two phases: (1) the liquid state covers over a length of 1.5 m behind the shield tail (phase 1), which is represented by a certain distributional pressure that acts on the ground surface and on the tunnel lining; (2) the solid state that is beyond this section (phase 2), in which the grout has been assumed to harden, and it has been simulated using perfect elastic volume elements, and with the elastic characteristics $E_{\text{grout}} = 10 \text{ MPa}$ and $\nu_{\text{grout}} = 0.22$ (Dias and Kastner 2013; Mollon et al. 2013). The migration of some grout towards the shield has been simulated by means of a triangular pressure over the length of one ring (1.5 m).

The tunnel segments have been modelled using a linear-elastic embedded liner element. The joints were simulated using double node connections, which allow the stiffness characteristics of the joint connection, represented by a set composed of a rotational spring, an axial spring and a radial spring (Do et al. 2013a, 2013c), to be taken into account.

A total weight of 3,980 kN has been simulated for the back-up train through the distribution loads which act on the lining elements at the bottom region of the tunnel over an assumed angle of 90° in the cross-section, and over a

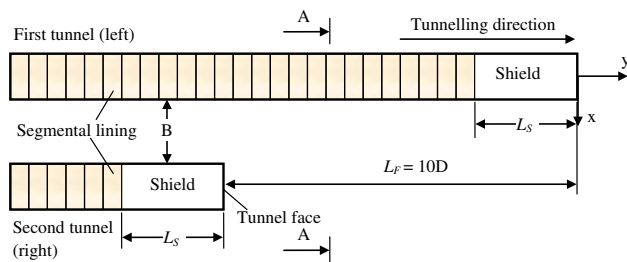


Fig. 1 Plan view of the twin tunnels (not scaled) (from Do et al. 2014)

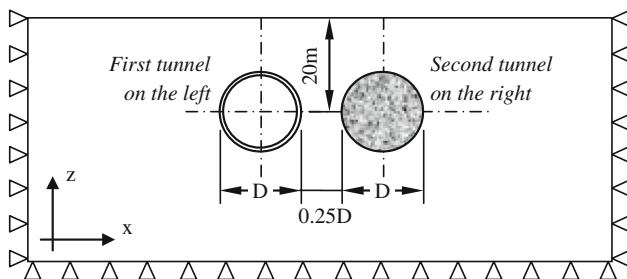


Fig. 2 A-A: typical cross-section view of the twin tunnels (not scaled) (from Do et al. 2014)

tunnel length of 72 m behind the shield tail (Kasper and Meschke 2004).

Owing to the fact that the results presented by Do et al. (2014) indicated a greater impact of the new tunnel excavation on the structural behaviour of the existing tunnel, in the case of twin tunnels excavated at a large lagged distance compared to that observed in the case of the simultaneous excavation of twin tunnels, the present study has only considered the former case. The twin tunnel excavation sequence has been modelled as follows: (1) excavation of the first tunnel (left); (2) excavation of the second tunnel (right) with a lagged distance L_F of $10D$ behind the face of the first tunnel, in which D is external excavation diameter of the tunnel. This lagged distance is large enough to consider that the settlement trough induced on the ground surface during the excavation of the first tunnel is not disturbed by the excavation of the second tunnel. Five cases of tunnel distance B , that is, $0.25D$, $0.5D$, $1D$, $1.5D$ and $2D$, were simulated. A plan view and typical cross-section of the twin tunnel excavation procedure are illustrated in Figs. 1 and 2.

Numerical results and discussion

This section deals with the variations in the lining forces developed in the tunnel linings and the ground

displacements over the tunnels during the excavation process of the new tunnel on the right. These variations were determined at the section corresponding to the 30th ring, counting from the model boundary ($y = 0$ m). The effect of the model boundary condition on the behaviour of the tunnels is negligible at this section (Do et al. 2013a, 2014).

Surface settlements

Figures 3 and 4 show the development of the surface settlement trough in the transverse section, caused by the excavation of the twin tunnels for tunnel distances of $0.25D$ and $2D$, respectively. The same settlement trough tendencies were also obtained for the other cases when the tunnel distances B was equal to $0.5D$, $1D$ and to $1.5D$. The meaning of each curve is given in Table 1.

First, the settlement troughs determined using the $FLAC^{3D}$ numerical model are analysed. As expected, on the basis of the work by the same authors (Do et al. 2014), the final settlement profiles are asymmetric. This means that the maximum settlement is not located over the mid-point between the two tunnels. Do et al. (2014) indicated that the two settlement troughs caused by the construction of the tunnels on the left and right have a similar shape. The settlement trough above the new tunnel on the right is determined by subtracting the settlement trough caused by the excavation of the existing tunnel on the left from the final settlement trough of the twin tunnels. The numerical results of the maximum settlements developed over the twin tunnels are presented in Table 2.

Figure 5 and Table 2 show the settlement ratios R_1 and R_2 , which are defined as the ratio of maximum settlements, determined after the excavation of the second tunnel, over the second tunnel and over the twin tunnels, respectively, on the maximum settlement value over the first tunnel before the passage of the second tunnel. It can be seen that, in all the considered cases, the additional settlements induced by the second tunnel are smaller or shallower than the settlements induced by the first tunnel. The same observation was also made for the field measurement introduced by Suwansawat and Einstein (2007), Chen et al. (2011) and He et al. (2012).

It is important to note that the closer the centres of the tunnels, the smaller the value of trough parameter i and the smaller the maximum settlement δ_{max2} observed above the new tunnel on the right. The increase in the maximum settlement δ_{max2} , as the tunnel distance B increases, could be attributed to the decrease effect of the first tunnel excavation on the second tunnel. However, the difference in the maximum additional settlement over the centreline of the second tunnel (δ_{max2}) in all the considered cases of tunnel distance B is insignificant. The R_1 ratio is approximately equal to about 80 % (see Table 2; Fig. 5).

Fig. 3 Comparison of the settlement troughs in the transverse section of the twin tunnels, for $B = 0.25D$ case (D is tunnel diameter in meters)

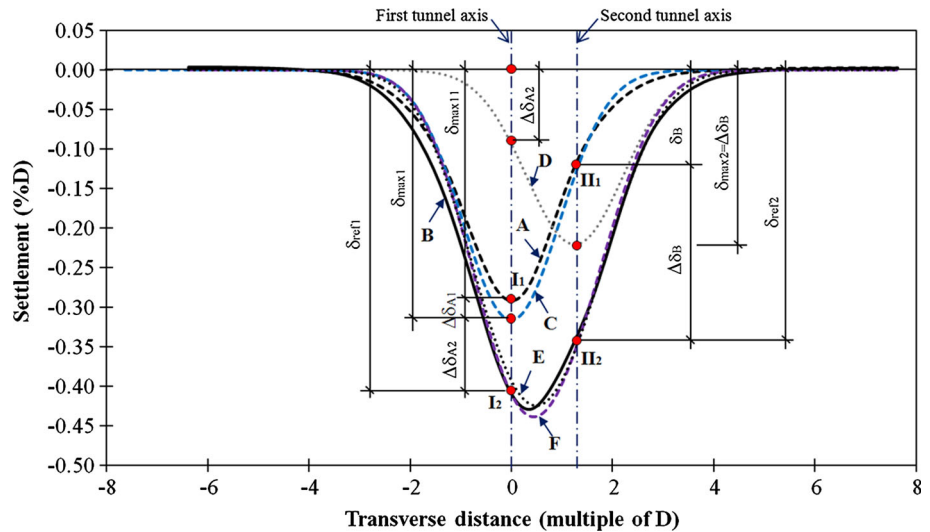


Fig. 4 Comparison of the settlement troughs in the transverse section of the twin tunnels, for $B = 2D$ case (D is tunnel diameter in meters)

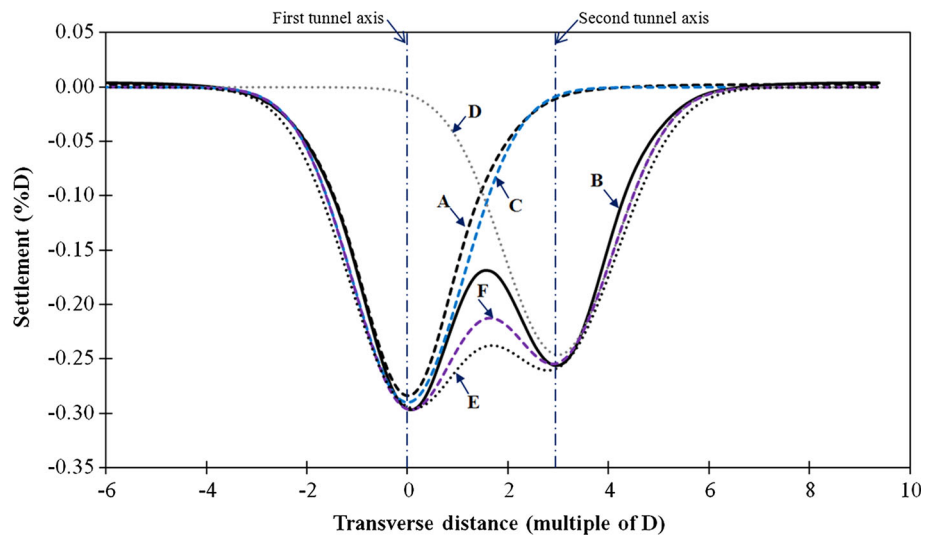


Table 1 Description of curves in Fig. 3

| Curve | Description |
|-------|--|
| A | Surface settlement curve caused by the excavation of the first single tunnel obtained with FLAC ^{3D} numerical model |
| B | Surface settlement curve over the twin tunnels after the excavation of the second tunnel obtained with FLAC ^{3D} numerical model |
| C | Surface settlement curve over the first tunnel after the excavation of the second tunnel determined using the modified procedure of the present study |
| D | Surface settlement curve over the second tunnel after the excavation of the second tunnel determined using the modified procedure of the present study |
| E | Surface settlement curve over the twin tunnels determined using the procedure proposed by Suwansawat and Einstein (2007) |
| F | Surface settlement curve over the twin tunnels determined using the modified procedure proposed of the present study |

As expected, when the distance of tunnel B increases, the settlement trough over the twin tunnels is shallower and wider at the final state (see Figs. 3, 4 and Table 2). Figure 5 indicates that the final maximum settlement over the twin tunnels decreases as the tunnel distance increases. Its value is somewhat similar to that of a single tunnel when tunnel distance B reaches about $2D$.

It is interesting to note that the total volume loss ratio at the final state, VL , over the twin tunnels, determined using the numerical models as the ratio of the settlement trough area developed on the ground surface to the cross-section area of the tunnel, is roughly similar in all the considered cases and approximately equal to 1.70 %. In other words, the additional volume loss caused by the excavation of the second tunnel does not seem to depend to a great extent on the distance between the two tunnels. It can instead be attributed to the fact that, in all

Table 2 Comparison of the surface settlements determined using numerical models

| | Distance B (multiple of D) | | | | |
|--|----------------------------|-------|-------|-------|-------|
| | 0.25 | 0.5 | 1 | 1.5 | 2 |
| Max. settlement over the first (single) tunnel δ_{max11} (% D)* | 0.265 | | | | |
| Max. settlement over the second tunnel δ_{max2} (% D)* | 0.220 | 0.221 | 0.223 | 0.236 | 0.246 |
| $R_1 = \frac{\delta_{max2}}{\delta_{max11}}$ (%) | 75.5 | 75.7 | 76.6 | 81.1 | 84.6 |
| Max. settlement over the twin tunnel δ_{max} (%D)* | 0.429 | 0.396 | 0.342 | 0.315 | 0.297 |
| $R_2 = \frac{\delta_{max}}{\delta_{max11}}$ (%) | 147.2 | 135.7 | 117.2 | 108.1 | 101.9 |
| i value of trough parameter in Gaussian curves ($\times H$) | | | | | |
| Suwansawat and Einstein (2007) | 0.48 | 0.55 | 0.52 | 0.54 | 0.56 |
| Modified procedure | 0.45 | 0.47 | 0.48 | 0.50 | 0.52 |
| Root Mean Square Error (RMSE) ($\times 10^{-4}$) | | | | | |
| Suwansawat and Einstein (2007) | 12.9 | 9.64 | 14.5 | 24.7 | 30.5 |
| Modified procedure | 13.3 | 9.83 | 9.84 | 15.2 | 19.2 |

*values obtained using FLAC^{3D} numerical model

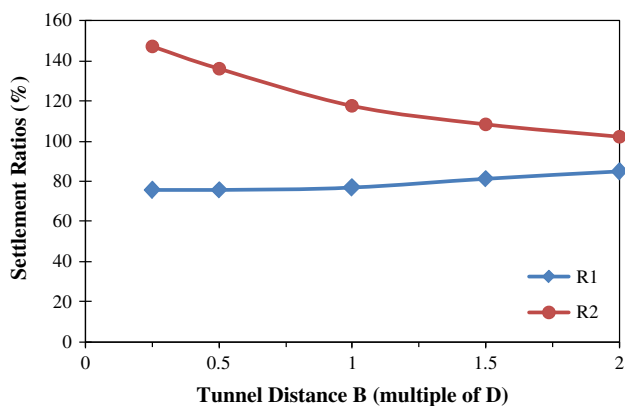


Fig. 5 The dependence of settlement ratios on the tunnel distance (D is tunnel diameter in meters)

the considered tunnel distance cases, the interference between the failure zones close to the two tunnels is not preponderant.

In addition to the surface settlement curves predicted using numerical models, the settlement troughs obtained using the superposition method proposed by Suwansawat and Einstein (2007) are also presented in these figures; this allows the applicability of the superposition method to be evaluated. It should be mentioned that the surface settlement trough over the first tunnel in the procedure proposed by Suwansawat and Einstein (2007) is considered constant and all of the additional surface settlement caused by the excavation of the second tunnel is only taken into account by means of the settlement trough of the second tunnel. In the present work, the following steps have been applied on the basis of the superposition procedure introduced by Suwansawat and Einstein (2007):

- Determination of the maximum surface settlement developed over the centreline of the first (left) tunnel (i.e., point I_1 (δ_{max11}) in Fig. 3) and description of the entire settlement trough induced by the first tunnel using the Gaussian function proposed by Peck (1969):

$$\delta_1 = \delta_{max11} \exp \left[-\frac{x^2}{2i_1^2} \right], \tag{1}$$

where δ_1 is the ground surface settlement over the first tunnel, m;

δ_{max11} is the maximum surface settlement on the first tunnel, m;

i_1 is the horizontal distance from the flexible point to the centreline of the first tunnel, m;

x is the horizontal distance from measured point to the centreline of the first tunnel, m.

- Calculation of the additional settlement over the centreline of the second tunnel on the right (i.e., the distance II_1II_2 (δ_{max2}) in Fig. 3), by subtracting the settlement determined after the first shield passage from the settlement measured after the second passage;
- Construction of the additional settlement trough induced by the second shield using the Gaussian curve (Eq. 2), and superimposition onto the settlement trough induced by the first shield to obtain the total settlement trough caused by the twin tunnels (Eq. 3).

$$\delta_2 = \delta_{max2} \exp \left[-\frac{(x - (B + D))^2}{2i_2^2} \right], \tag{2}$$

$$\begin{aligned} \delta &= \delta_1 + \delta_2 \\ &= \delta_{max11} \exp \left[-\frac{x^2}{2i_1^2} \right] + \delta_{max2} \exp \left[-\frac{(x - (B + D))^2}{2i_2^2} \right], \end{aligned} \tag{3}$$

where δ_2 is the ground surface settlement caused by the second tunnel after excavation of the second tunnel, m;

$\delta_{\max 2}$ is the maximum surface settlement caused by the second tunnel after excavation of the second tunnel, m;

δ is the ground surface settlement over the twin tunnels after excavation of the second tunnel, m;

i_2 is the horizontal distance from the flexible point to the centreline of the second tunnel, m;

B is the tunnel distance (see Fig. 2), m;

D is the diameter of the tunnel, m.

For simplification purpose, the same i values (i.e., i_1 and i_2) introduced in the above equations were adopted in the present study (e.g., Ocak 2014) and considered as an unknown parameter. Its value was chosen during the application of this superposition method on the basis of an optimization with the least squares method of the settlement over the centrelines of the two tunnels:

$$f(\delta_{\text{ref1}}, \delta_{\text{ref2}}) = (\delta_{\text{ref1-Gaussian}} - \delta_{\text{ref1-measured}})^2 + (\delta_{\text{ref2-Gaussian}} - \delta_{\text{ref2-measured}})^2, \tag{4}$$

where $\delta_{\text{ref1-Gaussian}}$, $\delta_{\text{ref2-Gaussian}}$ are the surface settlements at the centrelines of the first and second tunnels, respectively, which are estimated using Eq. (3) after excavation of the second tunnel, m;

$\delta_{\text{ref1-measured}}$, $\delta_{\text{ref2-measured}}$ are the measured surface settlements at the centrelines of the first and second tunnels, respectively, after excavation of the second tunnel, m.

The comparison results indicate that, as the tunnel distance B increases ($B = 2D$ case), a significant difference between the settlement curves, obtained using numerical models and the Gaussian method, can be seen at the region between the two tunnels (see Fig. 4). This means that, in the present studied case, the procedure proposed by Suwansawat and Einstein (2007) does not give a good approximation for the surface settlement trough at the zone between the two tunnels. The settlement troughs over each individual tunnel obtained using this procedure are not shown in Fig. 3 or Fig. 4 for simplification reason.

A modified procedure has been introduced in the present study. Unlike the procedure proposed by Suwansawat and Einstein (2007), the fundamental aspect of this modified procedure is the assumption that the excavation of the second tunnel, which is close to the first tunnel, causes a certain disturbance on the ground zone over the first (existing) tunnel. Consequently, in addition to a supplementary surface settlement developing over the second tunnel, which has been mentioned by many authors, a supplementary increase in the surface settlement trough over the first tunnel is also predicted. The supplementary increase in the surface settlement trough over the first tunnel can be explained by the additional large downward vertical movement of the first tunnel crown during the passage of the second tunnel, as indicated in the work by

Do et al. (2014), and can also be seen from the additional normal displacements of the first tunnel presented in Fig. 6. It should be noted that, all the settlement curves developed over each tunnel in this modified procedure have also been constructed using the Gaussian function proposed by Peck (1969).

On the basis of this finding, the following modified procedure can be suggested to describe the settlement troughs:

- Measure the surface settlement developed over the centreline of the first (left) tunnel (i.e., point I₁ (δ_A) in Fig. 3) and the settlement over the centreline of the second tunnel (i.e., point II₁ (δ_B) in Fig. 3); The maximum surface settlement caused by the first single tunnel $\delta_{\max 11}$ is equal to δ_A ;
- Measure the additional surface settlements developed over the two centrelines, that is, the distances $\Delta\delta_A$ and $\Delta\delta_B$ in Fig. 3, respectively, caused by the excavation of the second tunnel. The maximum settlement caused by only the second tunnel after excavation of the second tunnel ($\delta_{\max 2}$) is equal to $\Delta\delta_B$;
- It is reasonable to assume that the measured additional settlement over the centreline of the existing tunnel ($\Delta\delta_A$) is constituted by two parts, that is, a supplementary settlement of the surface settlement trough over the first (existing) tunnel ($\Delta\delta_{A1}$) and a

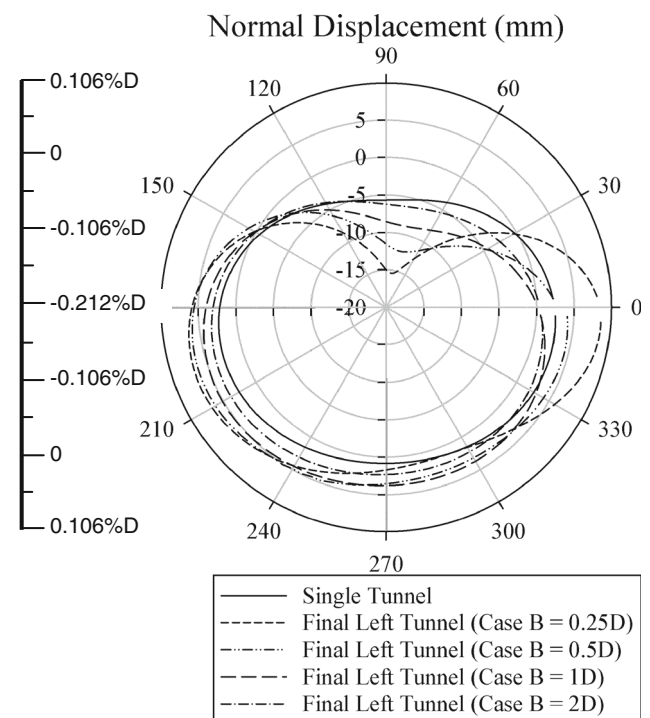


Fig. 6 Normal displacements in measured lining ring 30 of the existing tunnel on the left

new settlement of the new surface settlement trough that develops over the second tunnel ($\Delta\delta_{A2}$) (see Fig. 3). The maximum settlement caused by only the first tunnel after the excavation of the second tunnel ($\delta_{\max1}$) is equal to the sum of $\delta_{\max11}$ and $\Delta\delta_{A1}$ ($\delta_{\max1} = \delta_{\max11} + \Delta\delta_{A1} = \delta_A + \Delta\delta_{A1}$). In order to estimate the value of $\Delta\delta_{A1}$, it is necessary to know $\Delta\delta_{A2}$ ($\Delta\delta_{A1} = \Delta\delta_A - \Delta\delta_{A2}$). For this purpose, the distance from the flexible point of the surface settlement trough to the centreline of each tunnel (i.e., i_1 and i_2) is assumed to be the same. The best i value is obtained from an optimization, with the least squares method, of the settlements over the centrelines of the two tunnels (i.e., $\delta_{\text{ref}1}$ and $\delta_{\text{ref}2}$ in Fig. 3), using Eq. (4). It should be noted that the maximum surface settlement on the first tunnel, $\delta_{\max11}$, in Eq. (3) should be replaced by $\delta_{\max1}$. The maximum settlement over the second tunnel (i.e., $\delta_{\max2}$) is instead similar to that applied in the procedure by Suwansawat and Einstein (2007).

In order to evaluate the modified procedure, the Root Mean Square Error (RMSE) of the surface settlements was used to compare the quality of the fitting of these two methods (i.e. Suwansawat and Einstein 2007, and the modified procedure):

$$\text{RMSE} = \sqrt{\frac{\sum_{j=1}^k (S_j - \delta_j)^2}{k}}, \quad (5)$$

where S_j is the surface settlement of the j th point determined using the FLAC^{3D} numerical model, m ;

δ_j is the predicted surface settlement of the j th point determined from Eq. (3), m ;

k is the number of points in the settlement array.

The results shown in Table 2 indicate that, when the tunnel distance increases, the modified procedure gives a better surface settlement trough over the twin tunnels than that of Suwansawat and Einstein (2007). The difference in the predicted results obtained by these two procedures for small tunnel distances (e.g., $B = 0.25D$ and $B = 0.5D$) is insignificant.

It is interesting to note that, in all the considered cases, the i parameter obtained using the modified procedure is always smaller than the one determined using the Suwansawat and Einstein procedure. This could be attributed to the fact that, while the maximum settlement over the second tunnel is the same in both procedures, the maximum settlement over the first tunnel in the modified procedure (i.e., $\delta_{\max1}$ in Fig. 3), which is determined after the passage of the second tunnel, is greater than that of Suwansawat and Einstein (i.e., $\delta_{\max11}$ in Fig. 3).

Normal displacement in the tunnel lining

The positive and negative normal displacements, corresponding to the inward and outward deformations of the tunnel lining, are discussed in this section.

Figure 6 illustrates a significant effect of the tunnel distance on the deformation developed in the existing tunnel, due to the impact of the new tunnel. The large affected zones are located at the tunnel crown and at the spring line. As expected, the largest deformation induced in the existing tunnel linings, caused by the passage of the new tunnel, can be observed for the case of a tunnel distance B of $0.25D$ (see Fig. 6 and Table 3).

Unlike the existing tunnel, the normal deformation induced in the new tunnel lining is similar to that of a single tunnel for all the cases of tunnel distance B (see Fig. 7 and Table 4).

Normal forces and longitudinal forces in the tunnel lining

Figure 8a and Table 3 show a significant effect of the tunnel distance on the normal forces induced in the existing tunnel on the left at the final state, due to the impact of the new tunnel.

The excavation of a new tunnel generally causes an increase in the normal forces induced in the existing tunnel all around the tunnel (see Fig. 8a). The impact of the new tunnel is important, and in particular at the spring line on the right near the new tunnel.

Figure 8a also indicates that the greatest impact of the new tunnel on the existing tunnel can be observed in $B = 0.5D$ case, but not in $B = 0.25D$ case. This means that the largest transfer of the load from the new tunnel to the existing tunnel occurs at a medium distance of $B = 0.5D$. This observation could be explained by observing the interaction between the two mechanized tunnels during the advancement of the new tunnel. As described in detail in the work by the same authors (Do et al. 2014), in $B = 0.25D$ case, the greatest impact of the new tunnel on the existing tunnel, in terms of normal forces induced in the existing tunnel, can be observed when the face of the new tunnel approaches the measured section ($Y_{MS} = 0D$). However, in the case in which the tunnel distance of B is larger than $0.25D$, the numerical results obtained in the present study indicate that the greatest impact of the new tunnel on the normal forces induced in the existing tunnel do not occur at the moment corresponding to $Y_{MS} = 0D$, but at the moment when the shield in the new tunnel passes over the measured section ($Y_{MS} = 3D$). At this moment ($Y_{MS} = 3D$), the increase in the normal forces induced in the existing tunnel lining could be attributed to the movement of the ground at the

Table 3 Development of the structural forces and deformation in measured ring 30 in the existing tunnel on the left

| Parameters | Single tunnel | Tunnel distance B (multiple of tunnel diameter (D) in meter) | | | | |
|----------------------------------|---------------|--|--------|-------|-------|-------|
| | | 0.25 | 0.5 | 1 | 1.5 | 2 |
| Max. pos. bending moment (kNm/m) | 71.9 | 348.1 | 166.1 | 67.8 | 58.7 | 56.7 |
| R_{M+} (%) | 100 | 483.8 | 230.9 | 94.3 | 81.6 | 78.8 |
| Min. neg. bending moment (kNm/m) | -93.8 | -480.6 | -273.5 | -93.0 | -83.3 | -80.0 |
| R_{M-} (%) | 100 | 512.0 | 291.4 | 99.1 | 88.8 | 85.3 |
| Max. Normal force (kN/m) | 1,490 | 1,927 | 2,141 | 1,844 | 1660 | 1,559 |
| $R_{N_{max}}$ (%) | 100 | 129.3 | 143.7 | 123.8 | 111.4 | 104.6 |
| Min. Normal force (kN/m) | 468 | 553 | 542 | 509 | 489 | 477 |
| $R_{N_{min}}$ (%) | 100 | 118.1 | 115.8 | 108.7 | 104.5 | 101.9 |
| Max. Longitudinal force (kN/m) | 1745 | 1798 | 1787 | 1737 | 1728 | 1 718 |
| R_{LN} (%) | 100 | 103.0 | 102.4 | 99.5 | 99.0 | 98.4 |
| Max. normal displacement (mm) | 5.69 | 15.42 | 12.32 | 8.89 | 7.31 | 6.33 |
| R_{disp+} (%) | 100 | 271.2 | 2-16.6 | 156.3 | 128.5 | 111.4 |
| Min. normal displacement (mm) | -2.78 | -8.65 | -6.33 | -5.11 | -4.30 | -3.82 |
| R_{disp-} (%) | 100 | 310.8 | 227.4 | 183.7 | 154.7 | 137.4 |

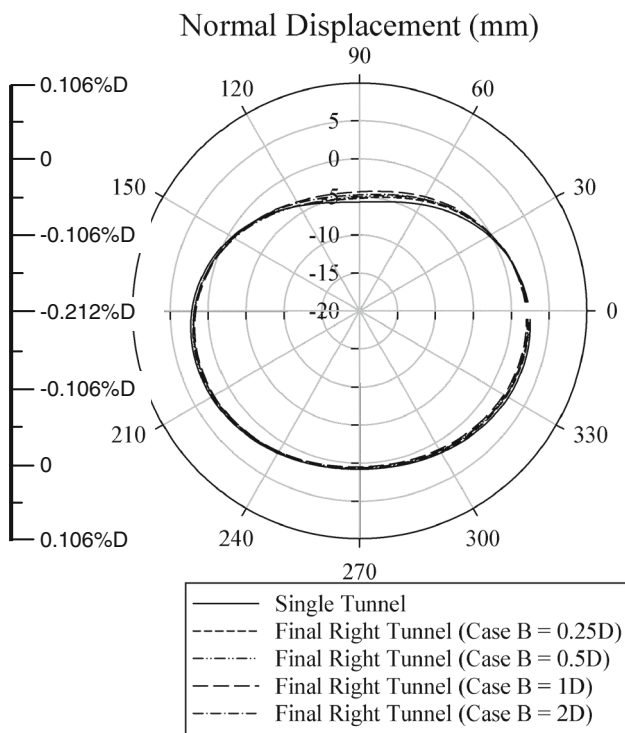


Fig. 7 Normal displacements in measured lining ring 30 of the new tunnel on the right

region between the two tunnels, from the new tunnel to the existing tunnel, due to the low value of the lateral earth coefficient ($K_0 = 0.5$) in the studied case. This movement caused a load transfer from the new tunnel to

the existing tunnel that led to an increase in the normal forces measured at the spring line on the right in the existing tunnel near the new tunnel (Do et al. 2014). Consequently, in spite of the increase in tunnel distance B, the maximum normal force developed in the existing tunnel at the spring line on the right, in $B = 0.5D$ case, and at the final state, is still larger than that obtained in $B = 0.25D$ case. Beyond a tunnel distance of $B = 0.5D$, the normal forces developed at the spring line on the right in the existing tunnel decrease. This could be explained by the decrease in the interaction between the two tunnels.

The maximum normal forces obtained in $B = 0.5D$ case are different from those observed after the 2D numerical calculations considered by the same authors (Do et al. 2013b), in which a gradual decrease in the effect of the new tunnel on the normal forces induced in the existing tunnel as the tunnel distance B increases was observed. This difference highlights the necessity of using a 3D calculation to estimate the interaction between tunnels.

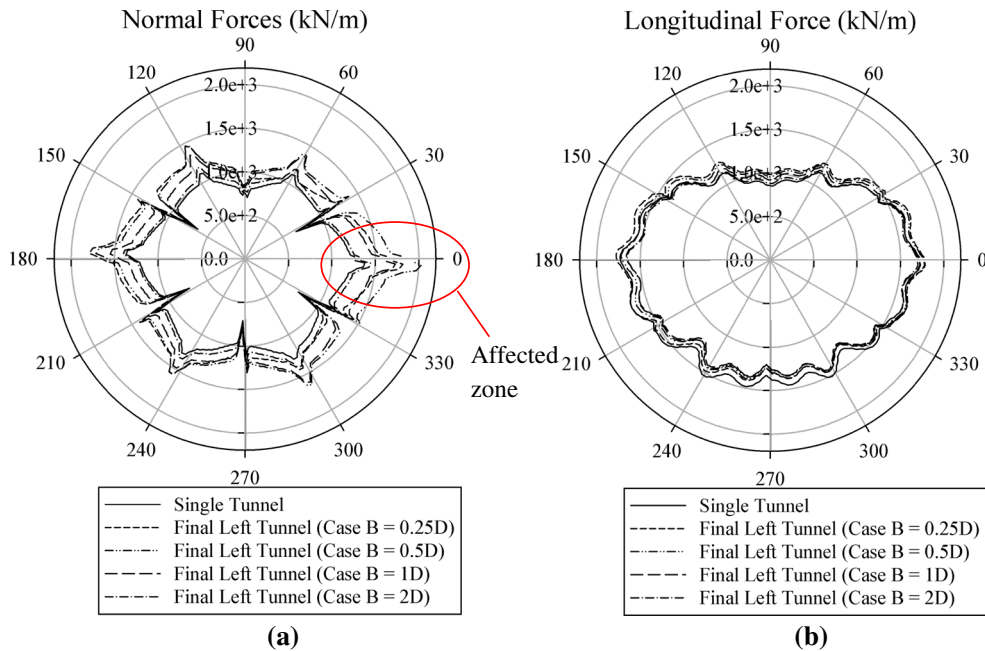
Unlike the normal forces in the existing tunnel on the right side near the new tunnel, and as expected, on the left side of the existing tunnel where small impacts of the excavation of the new tunnel have been predicted, the larger the tunnel distance B, the smaller the increase in normal forces induced in the existing tunnel (see Fig. 8a). As for the longitudinal forces at the final state, Fig. 8b illustrates an insignificant effect of the interaction between the two tunnels.

Figure 9 shows the distribution of the normal force and longitudinal force in the new tunnel on the right. It can be

Table 4 Development of the structural forces and deformation in measured ring 30 in the new tunnel on the right

| Parameters | Single tunnel | Tunnel distance B (multiple of tunnel diameter (D) in meters) | | | | |
|----------------------------------|---------------|---|-------|-------|-------|-------|
| | | 0.25 | 0.5 | 1 | 1.5 | 2 |
| Max. pos. bending moment (kNm/m) | 71.9 | 65.8 | 60.8 | 58.4 | 58.3 | 60.2 |
| R_{M+} (%) | 100 | 91.5 | 84.5 | 81.2 | 81.0 | 83.7 |
| Min. neg. bending moment (kNm/m) | -93.8 | -89.9 | -90.7 | -78.2 | -78.0 | -83.1 |
| R_{M-} (%) | 100 | 95.8 | 96.6 | 83.4 | 83.1 | 88.5 |
| Max. Normal force (kN/m) | 1490 | 1491 | 1479 | 1441 | 1442 | 1 451 |
| $R_{N_{max}}$ (%) | 100 | 100.1 | 99.3 | 96.7 | 96.8 | 97.4 |
| Min. Normal force (kN/m) | 468 | 469 | 467 | 458 | 461 | 460 |
| $R_{N_{min}}$ (%) | 100 | 100.2 | 99.8 | 97.8 | 98.5 | 98.2 |
| Max. Longitudinal force (kN/m) | 1745 | 1667 | 1670 | 1667 | 1683 | 1 715 |
| R_{LN} (%) | 100 | 95.5 | 95.7 | 95.5 | 96.4 | 98.2 |
| Max. normal displacement (mm) | 5.69 | 5.24 | 5.08 | 4.40 | 4.52 | 4.80 |
| R_{disp+} (%) | 100 | 92.1 | 89.2 | 77.3 | 79.5 | 84.4 |
| Min. normal displacement (mm) | -2.78 | -2.51 | -2.45 | -2.20 | -2.24 | -2.34 |
| R_{disp-} (%) | 100 | 90.1 | 88.0 | 79.1 | 80.6 | 84.3 |

Fig. 8 Normal force and longitudinal force of the existing tunnel lining on the left. **a** Normal force in measured lining ring 30 of the existing tunnel on the left. **b** Longitudinal force in measured lining ring 30 of the existing tunnel on the left



seen that these forces in the new tunnel are not affected to any great extent by the presence of the existing tunnel on the left, regardless of tunnel distance B.

Bending moment in the tunnel lining

Figure 10 shows the distribution of the bending moment induced in the existing tunnel on the left for different tunnel distances. It can be seen that the effect of the new tunnel excavation on the right on the bending moment induced in the existing tunnel, in particular on the right side near the new tunnel, depends to a great extent on tunnel

distance B. As expected, the smaller the tunnel distance B, the larger the increase in the bending moment developed in the existing tunnel caused by the impact of the new tunnel. The increase in the bending moment in the lining of the existing tunnel, when tunnel distance B is smaller than 1D, could mainly be attributed to the loss in ground surrounding the new tunnel, which is then followed by the downward movement of the ground above the existing tunnel as can be seen in Sects. 3.1, 3.2 of this study and also explained by Do et al. (2014). This effect decreases as the tunnel distance increases, and this could help to explain the gradual decrease in the bending moment in the existing

Fig. 9 Normal force and longitudinal force of the new tunnel lining on the right. **a** Normal force in measured lining ring 30 of the new tunnel on the right. **b** Longitudinal force in measured lining ring 30 of the tunnel on the right

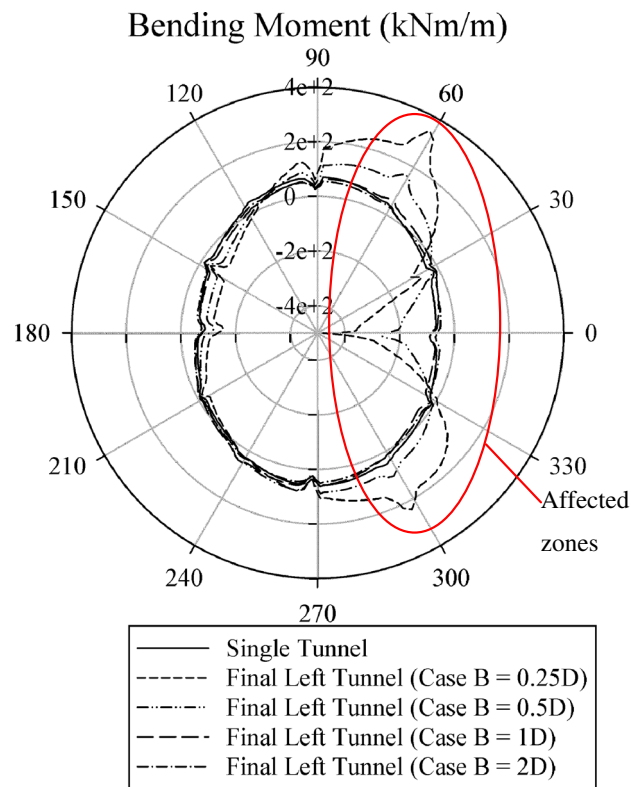
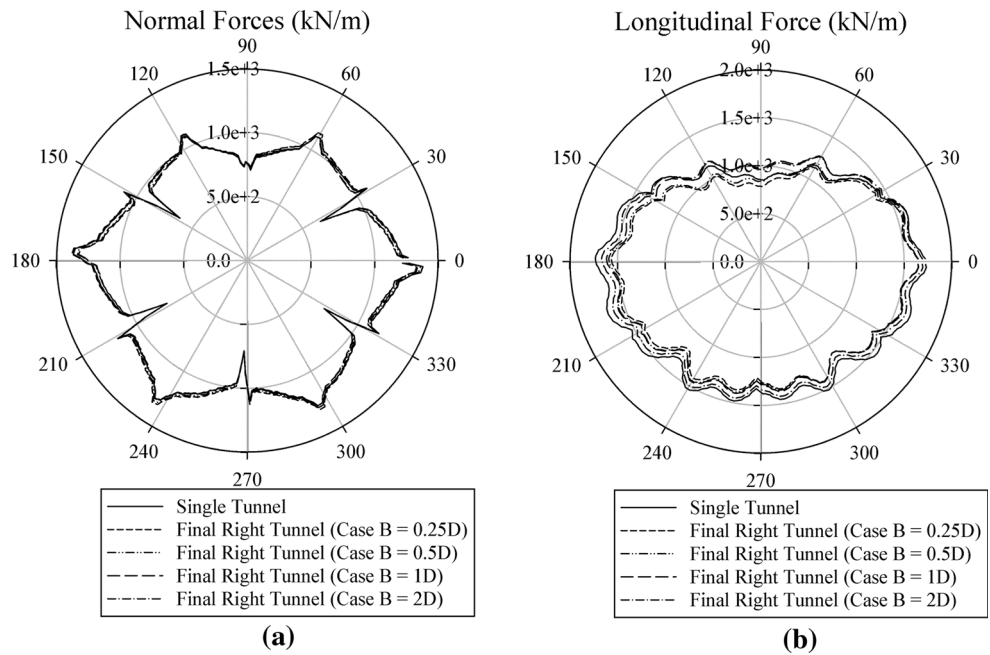


Fig. 10 Bending moment in measured lining ring 30 of the existing tunnel on the left

tunnel as a function of the tunnel distance. However, the excavation of the new tunnel beyond a tunnel distance of about 1D is followed by a slight decrease in the bending moment that is induced in the existing tunnel, compared to that of a single tunnel (see Fig. 10; Table 3). This decrease

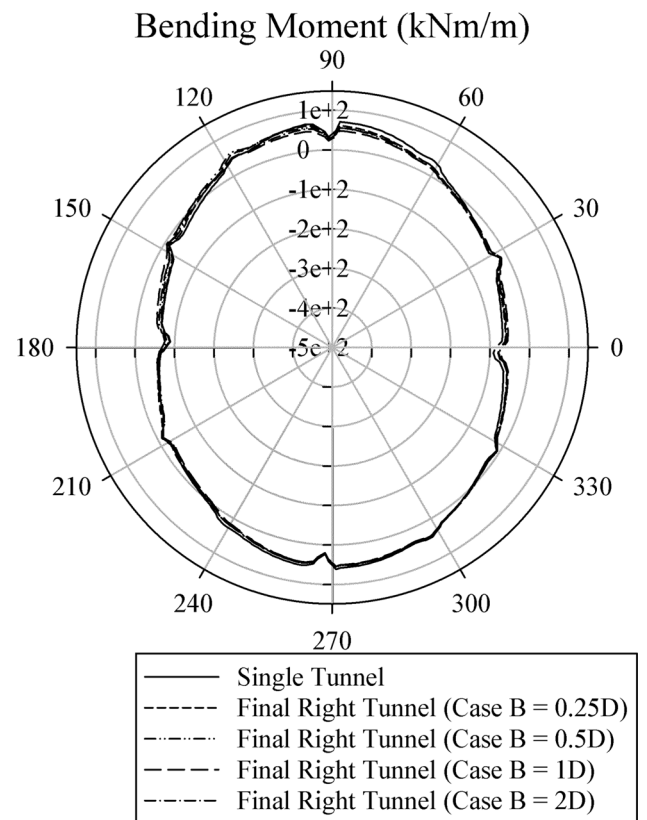


Fig. 11 Bending moment in measured lining ring 30 of the new tunnel on the right

could be attributed to the movement of the ground from the new tunnel towards the existing tunnel when the shield in the new tunnel passes over the measured section in the existing tunnel, due to the low value of the lateral earth

pressure coefficient ($K_0 = 0.5$) (see Do et al. 2014). This movement causes a load transfer from the new tunnel to the existing tunnel, which leads to a decrease in the ovaling loads around the existing tunnel and therefore to a decrease in the bending moments. It should be noted that the same effect of tunnel distance B on the bending moment induced in the existing tunnel was also observed when 2D numerical calculations were conducted by the same authors (Do et al. 2013b).

Table 4 and Fig. 11 show that, unlike in the existing tunnel on the left, the bending moment induced in the new tunnel on the right is generally smaller than that developed in a single tunnel. Owing to the construction of the first tunnel, the ground surrounding this tunnel is disturbed and reaches a new equilibrium state. The displacements of the ground are normally followed by a relaxation and redistribution of the stresses in the surrounding ground. These processes help to explain the above mentioned decrease in the bending moments induced in the lining of the second tunnel.

From the design point of view, it is reasonable to note that the critical distance of the interaction between the two horizontal tunnels, in terms of the bending moment, is equal to $1D$. This value is smaller than that applied to the surface settlement observed in Section 3.1.

Conclusions

In this study, a 3D numerical investigation of mechanized twin tunnels has been conducted which has allowed the effect of the tunnel distance between two horizontal tunnels on their structural behaviour and on the displacements field surrounding the tunnels to be highlighted. A modification of the superposition method introduced by Suwansawat and Einstein (2007) has been introduced. The results indicate that, for the cases studied in this paper, the modified procedure gives a good prediction of the surface settlement trough developed over twin horizontal tunnels. On the basis of 3D numerical analyses, it is possible to draw the following conclusions:

- (1) The superposition method can be used to obtain a preliminary estimation of the settlement curves above horizontal twin tunnels;
- (2) The settlement profile is asymmetric over the centreline of the pillar;
- (3) The existing tunnel is affected to a great extent by the construction of the second tunnel. However, the existing tunnel only causes a slight impact on the new tunnel. The behaviour of the new tunnel is similar to that of a single tunnel;

- (4) The critical distance between the two horizontal tunnels studied in this case is about a tunnel diameter;
- (5) The maximum normal force in $B = 0.5D$ case is greater than that obtained in $B = 0.25D$ case, which highlights the necessity of using a 3D simulation to estimate the interaction between tunnels.

Experimental studies will be necessary in the future to validate the numerical results obtained in this study.

Highlights

A modification applied to the superposition method has been presented;

The superposition method can be used to obtain a preliminary estimation of settlement curves above horizontal twin tunnels;

The critical distance between the two horizontal tunnels studied in this case is about a tunnel diameter;

The settlement profile is asymmetric over the centreline of the pillar;

The behaviour of the new tunnel is similar to that of a single tunnel.

References

- Chakeri H, Hasanpour R, Hindistan MA, Ünver B (2011) Analysis of interaction between tunnels in soft ground by 3D numerical modelling. *Bull Eng Geol Environ* 70:439–448
- Chen RP, Zhu J, Liu W, Tang XW (2011) Ground movement induced by parallel EPB tunnels in silty soils. *Tunn Undergr Space Technol* 26:163–171
- Chen SL, Gui MW, Yang MC (2012) Applicability of the principle of superposition in estimating ground surface settlement of twin- and quadruple-tube tunnels. *Tunn Undergr Space Technol* 28:135–149
- Dias D, Kastner R (2013) Movements caused by the excavation of tunnels using face pressurized shields - Analysis of monitoring and numerical modeling results. *Eng Geol* 152:17–25. doi:10.1016/j.enggeo.2012.10.002
- Dias D, Kastner R, Maghazi M (2000) Three dimensional simulation of slurry shield tunnelling. In: Kusakabe O, Fujita K, Miyazaki Y (eds) *Geotechnical aspects of underground construction in soft ground*. Balkema, Rotterdam, pp 351–356
- Do NA, Dias D, Oreste PP and Djeran-Maigre I (2013a) Three-dimensional numerical simulation for mechanized tunnelling in soft ground: the influence of the joint pattern. *Acta Geotechnica*, doi 10.1007/s11440-013-0279-7 (in press)
- Do NA, Dias D, Oreste PP, Djeran-Maigre I (2013b) Two-dimensional numerical investigation of twin tunnel interaction. *Geomech Eng* 6(3):263–275
- Do NA, Dias D, Oreste PP, Djeran-Maigre I (2013c) 2D numerical investigation of segmental tunnel lining behaviour. *Tunn Undergr Space Technol* 37:115–127

- Do NA, Dias D, Oreste PP, Djeran-Maigre I (2014) Three-dimensional numerical simulation for a twin mechanized tunnelling in soft ground. *Tunn Undergr Space Technol* 42:40–51
- Ercelebi SG, Copour H, Ocak I (2011) Surface settlement predictions for Istanbul metro tunnels excavated by EPB-TBM. *Environ Earth Sci* 62:357–365
- Hage Chehade F, Shahroui I (2008) Numerical analysis of the interaction between twin-tunnels: Influence of the relative position and construction procedure. *Tunn Undergr Space Technol* 23:210–214
- He C, Feng K, Fang Y, Jiang YC (2012) Surface settlement caused by twin-parallel shield tunnelling in sandy cobble strata. *J Zhejiang Univ Sci A Appl Phy Eng* 13(11):858–869 (ISSN 1673-565X Print; ISSN 1862-1775 Online)
- Hefny AM, Chua HC, Zhao J (2004) Parametric studies on the interaction between existing and new bored tunnels. *Tunn Undergr Space Technol* 19:471
- Itasca Consulting Group (2009) *FLAC Fast Lagrangian Analysis of Continua, Version 4.0. User's manual*
- Jenck O, Dias D (2004) Analyse tridimensionnelle en différences finies de l'interaction entre une structure en béton et le creusement d'un tunnel à faible profondeur. *Géotechnique* 54(8):519–528
- Kasper T, Meschke G (2004) A 3D finite element simulation model for TBM tunnelling in soft ground. *Int J Numer Anal Meth Geomech* 28:1441–1460
- Mollon G, Dias D, Soubra AH (2013) Probabilistic analyses of tunnelling-induced ground movements. *Acta Geotech* 8:181–199. doi:10.1007/s11440-012-0182-7
- Ocak I (2009) Environmental effects of tunnel excavation in soft and shallow ground with EPBM: the case of Istanbul. *Environ Earth Sci* 59:347–352. doi:10.1007/s12665-009-0032-6
- Ocak I (2014) A new approach for estimating the transverse surface settlement curve for twin tunnels in shallow and soft soils. *Environ Earth Sci*, doi: 10.1007/s12665-014-3145-5
- Ocak I, Seker SE (2013) Calculation of surface settlements caused by EPBM tunneling using artificial neural network, SVM, and Gaussian processes. *Environ Earth Sci* 70:1263–1276
- Peck RB (1969) Deep excavations and tunneling in soft ground: state-of-the-art report. In: Balkema AA Proceedings of 7th International Conference Soil Mechanics and Foundation Engineering, Mexico City, Rotterdam, The Netherlands, pp. 225–290
- Suwansawat S, Einstein HH (2007) Describing settlement troughs over twin tunnels using a superposition technique. *J Geotech Geoenviron Eng* 133(4):445–468